A comprehensive model for the synthesis of γ-Al_2O_3 microsphere supported bimetallic iron- and copper oxide materials

Bram Seynnaeve[1], Jeroen Lauwaert[1], Pascal Van Der Voort[2], An Verberckmoes[1]*

[1]Industrial Catalysis and Adsorption Technology, Department of Materials Textiles and Chemical Engineering, Ghent University, Valentin Vaerwyckweg 1, 9000 Ghent, Belgium

[2]Center for Ordered Materials, Organometallics and Catalysis, Department of Chemistry, Ghent University, Krijgslaan 281, 9000 Ghent, Belgium

*Address correspondence to Seynnaeve Bram, Bram.Seynnaeve@Ugent.be

Supporting Information

Table SI-1: Iron and copper loadings of each material, as experimentally determined with ICP-OES.

	Fe (wt%)	*Cu (wt%)*
Sim_Fe(NO₃)₃_Cu(NO₃)₂	3.94	3.98

Seq_ $Fe(NO_3)_3$_$Cu(NO_3)_2$	4.12	4.60
Seq_$Cu(NO_3)_2$_ $Fe(NO_3)_3$	4.15	4.24
Sim_$FeCl_3$_$Cu(NO_3)_2$	4.16	4.22
Seq_$FeCl_3$_$Cu(NO_3)_2$	4.48	4.47
Seq_$Cu(NO_3)_2$_$FeCl_3$	4.13	4.12
Sim_FeCitrate_$Cu(NO_3)_2$	4.11	4.42
Seq_FeCitrate_$Cu(NO_3)_2$	3.60	7.15
Seq_$Cu(NO_3)_2$_FeCitrate	3.00	4.50
Sim_$Fe(NO_3)_3$+HNO_3_$Cu(NO_3)_2$	4.53	4.63
Seq_$Fe(NO_3)_3$+HNO_3_$Cu(NO_3)_2$	4.30	4.73
Seq_$Cu(NO_3)_2$_$Fe(NO_3)_3$+HNO_3	3.80	3.76
Sim_$FeCl_3$+HCl_$Cu(NO_3)_2$	4.51	4.45
Seq_$FeCl_3$+HCl_$Cu(NO_3)_2$	6.12	4.81
Seq_$Cu(NO_3)_2$_$FeCl_3$+HCl	4.96	3.40
Seq_HCl-pretreatement+$FeCl_3$_ $Cu(NO_3)_2$	4.63	4.14
Seq_$Cu(NO_3)_2$_ HCl-pretreatement+$FeCl_3$	4.58	4.63

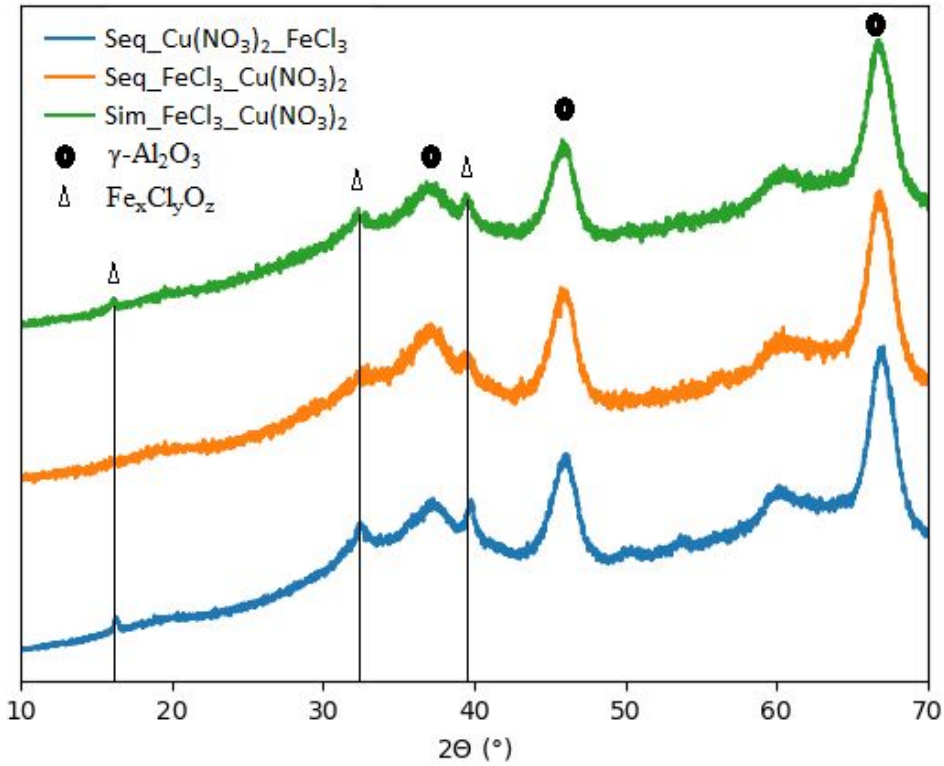

Figure SI-1: PXRD patterns of the bimetallic materials synthesized with $FeCl_3$ as iron source, with the diffractions of γ-Al_2O_3 and the unknown Fe-O-Cl compound marked

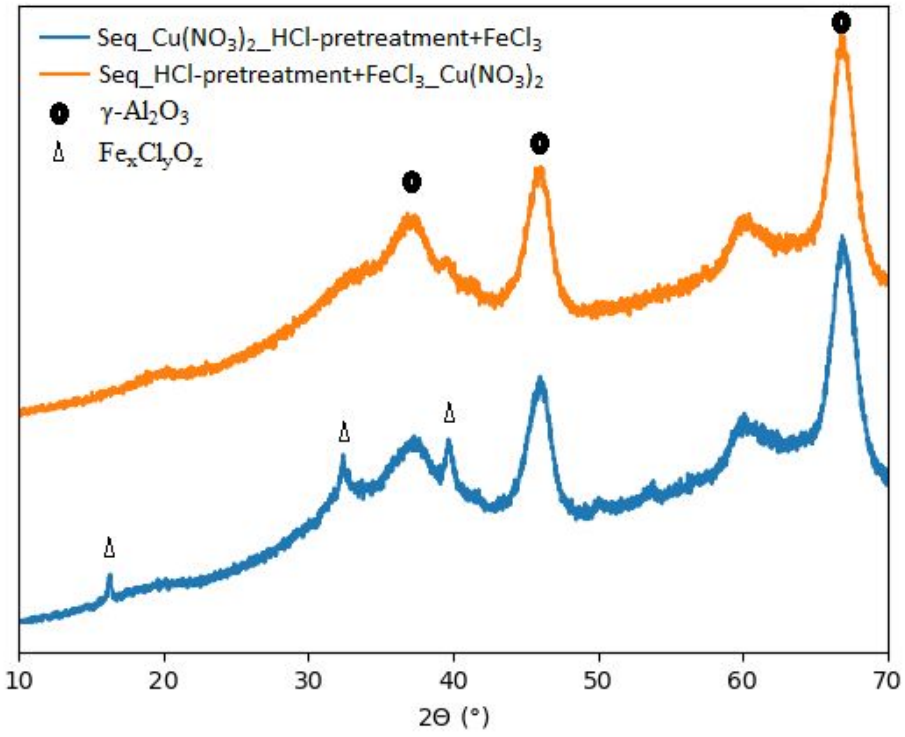

Figure SI-2: PXRD patterns of the bimetallic materials synthesized where HCl pretreatment was used, with the diffractions of γ-Al_2O_3 and the unknown Al-O-Cl compound marked

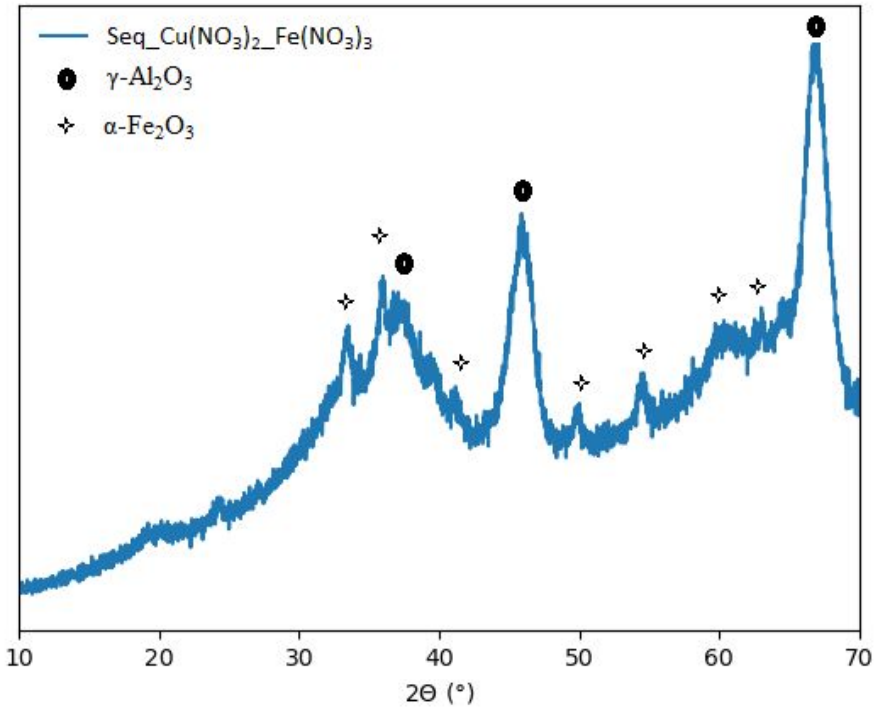

Figure SI-3: PXRD pattern of the seq_CuNO3_FeNO3 bimetallic material, with the diffractions of γ-Al_2O_3 and α-Fe_2O_3 marked

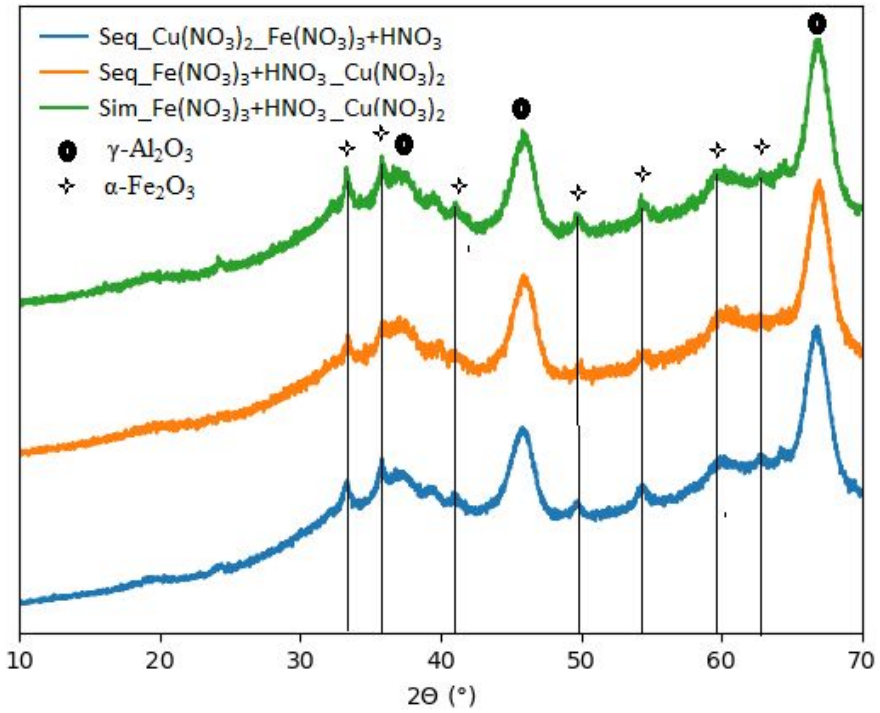

Figure SI-4: PXRD patterns of the bimetallic materials synthesized with $Fe(NO_3)_3$, acidified with HNO_3, as iron source, with the diffractions of γ-Al_2O_3 and α-Fe_2O_3 marked

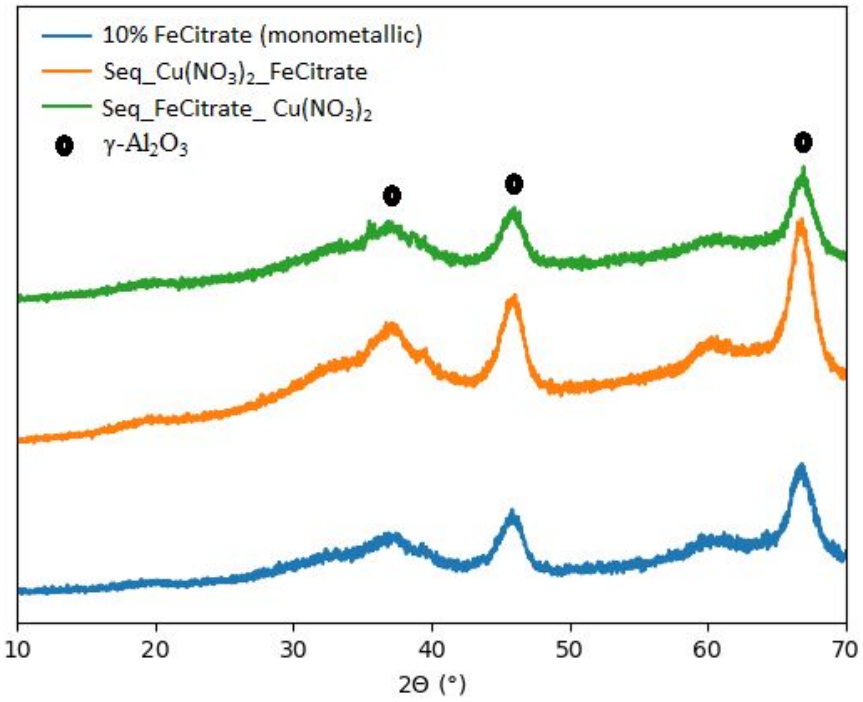

Figure SI-5: PXRD patterns of the bimetallic materials synthesized with ferric ammonium citrate as iron source, with a monometallic 10% iron oxide@Al_2O_3 made using ferric ammonium citrate as reference. The diffractions of γ-Al_2O_3 are marked

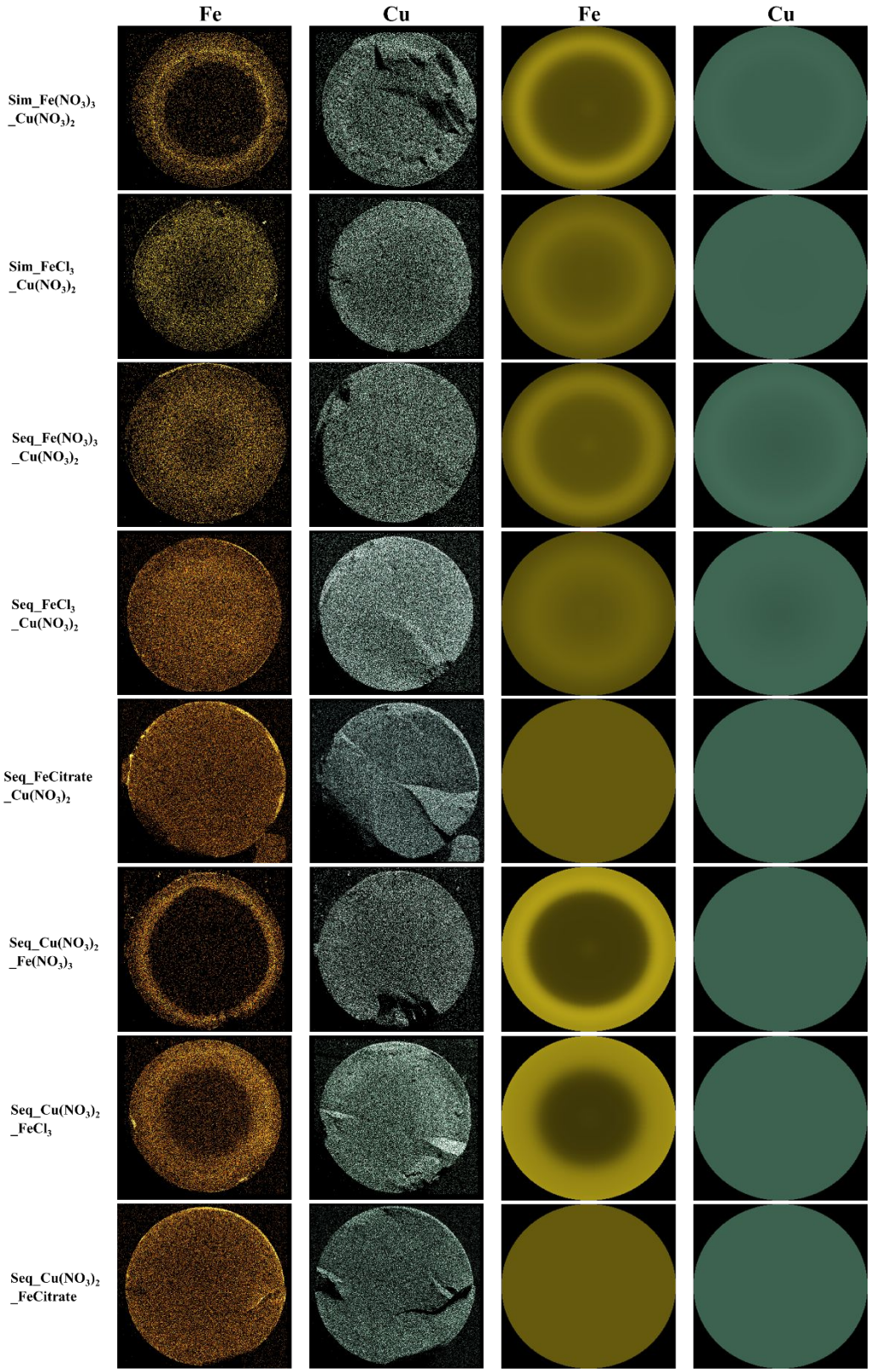
Fe
Cu
Fe
Cu
Sim_Fe(NO3)3 _Cu(NO3)2
Sim_FeCl3 _Cu(NO3)2
Seq_Fe(NO3)3 _Cu(NO3)2
Seq_FeCl3 _Cu(NO3)2
Seq_FeCitrate _Cu(NO3)2
Seq_Cu(NO3)2 _Fe(NO3)3
Seq_Cu(NO3)2 _FeCl3
Seq_Cu(NO3)2 _FeCitrate

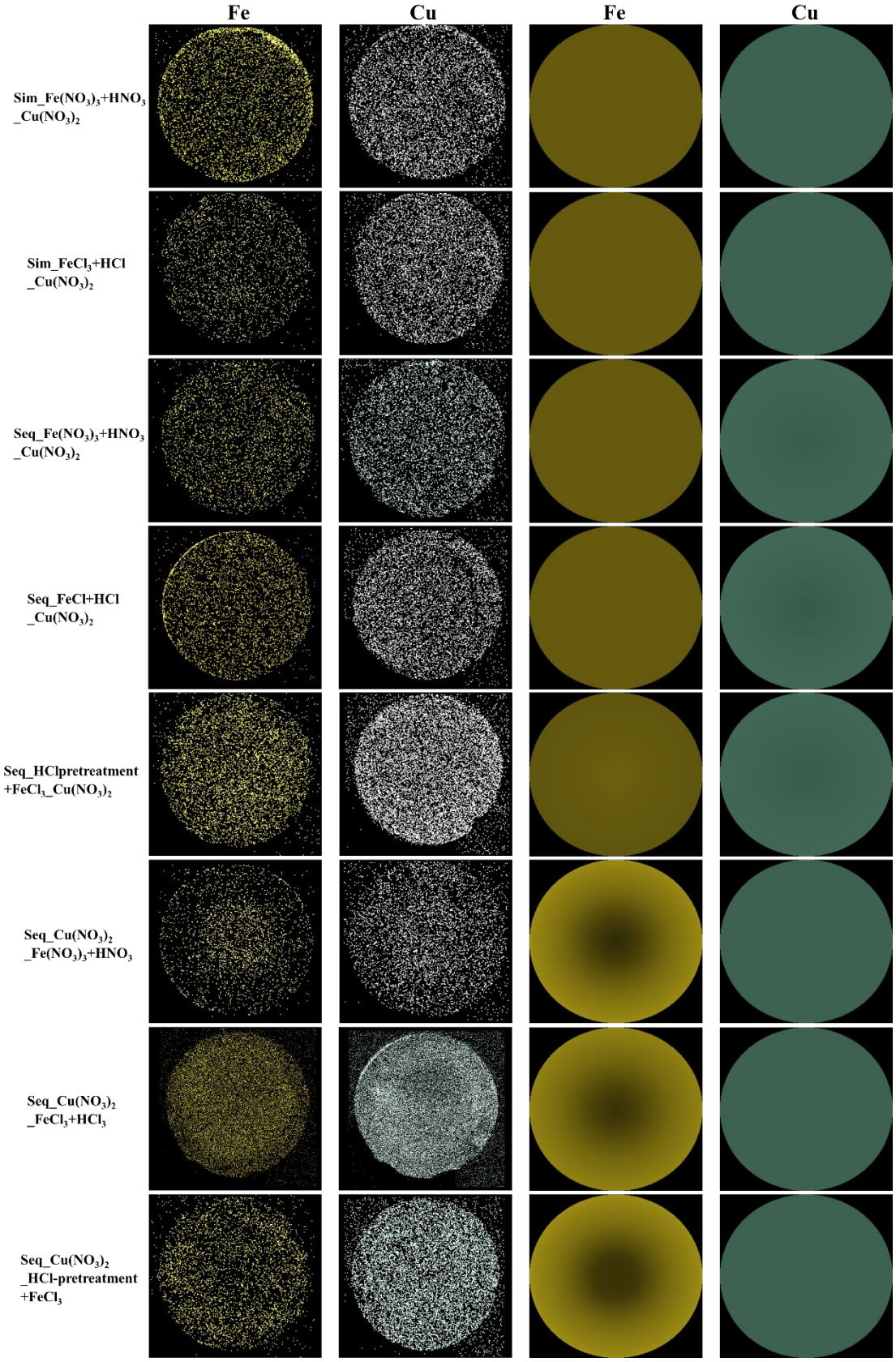
Fe
Cu
Fe
Cu
Sim_Fe(NO3)3+HNO3 _Cu(NO3)2
Sim_FeCl3+HCl _Cu(NO3)2
Seq_Fe(NO3)3+HNO3 _Cu(NO3)2
Seq_FeCl+HCl _Cu(NO3)2
Seq_HClpretreatment +FeCl3_Cu(NO3)2
Seq_Cu(NO3)2 _Fe(NO3)3+HNO3
Seq_Cu(NO3)2 _FeCl3+HCl3
Seq_Cu(NO3)2 _HCl-pretreatment +FeCl3

Figure SI-6: SEM-EDX mappings for each sample of the iron and copper distribution throughout an intersection of support microsphere (left), and the simulated iron and copper distributions predicted by the model (right)

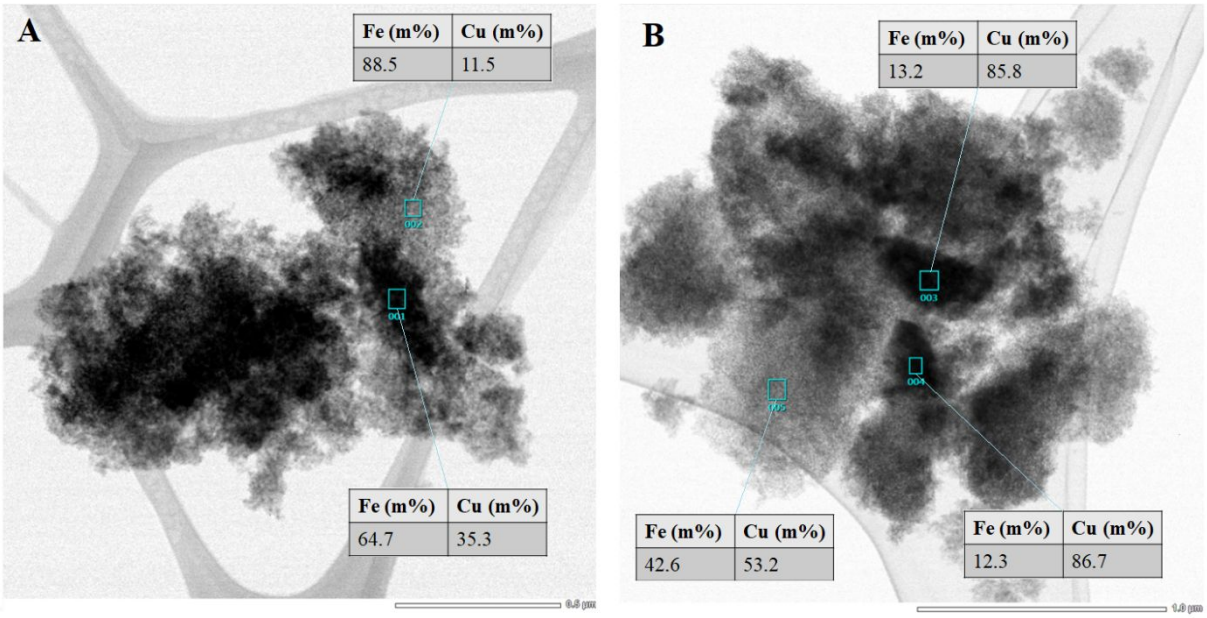

Figure SI-7: STEM images with Cu/Fe-EDX measurements of selected points, of alumina flakes of A. $1FeCl_3$+$2CuNO_3$ and B. $1CuNO_3$+$2FeCl_3$ materials. Darker areas correspond to alumina with more deposited metal and lighter areas correspond with alumina with little metal deposition